

Fast and accurate solvers for time-space fractional diffusion problem with spectral fractional Laplacian

Yi Yang^a, Jin Huang^{a,*}

^a*School of Mathematical Sciences, University of Electronic Science and Technology of China, Chengdu, 611731, China*

Abstract

This paper develops fast and accurate linear finite element method and fourth-order compact difference method combined with matrix transfer technique to solve high dimensional time-space fractional diffusion problem with spectral fractional Laplacian in space. In addition, a fast time stepping $L1$ scheme is used for time discretization. We can exactly evaluate fractional power of matrix in the proposed schemes, and perform matrix-vector multiplication by directly using a discrete sine transform and its inverse transform, which doesn't need to resort to any iteration method and can significantly reduce computation cost and memory. Further, we address the convergence analyses of full discrete scheme based on two types of spatial numerical methods. Finally, ample numerical examples are delivered to illustrate our theoretical analyses and the efficiency of the suggested schemes.

Keywords: Fractional diffusion problem, Spectral fractional Laplacian, Finite element method, Compact difference method, Matrix transfer technique, Convergence analysis

1. Introduction

Diffusion phenomena are ubiquitous [1–6]. From a microscopic point of view, the types of diffusion are usually classified according to the relation of the mean squared displacement of a particle to the time t , i.e., $\langle |x(t)|^2 \rangle \sim t^\beta$, $\beta > 0$ and $x(t)$ is the trajectory of a particle or a stochastic process. If $\beta = 1$, the process is normal diffusion; otherwise, the corresponding diffusion is called anomalous diffusion [6, 7].

Assume that Ω is a bounded region, $B(t)$ is a Brownian motion with $B(0) \in \Omega$, and $\tau_\Omega = \inf\{t : t > 0, B(t) \notin \Omega\}$. Given the s -stable subordinator T_t , a stochastic process can be defined by [8]

$$x(t) = \begin{cases} B(T_t), & T_t < \tau_\Omega, \\ \Theta, & T_t \geq \tau_\Omega, \end{cases}$$

where Θ is a coffin state. The process implies that the subordinated Brownian motion will be killed when particle first leaves Ω . In addition, the infinitesimal generator of $x(t)$ possesses the form [8–10]

$$(-\Delta)^s u(\mathbf{x}, t) = \sum_{j=1}^{\infty} (u, \varphi_j) \lambda_j^s \varphi_j, \quad (1)$$

where $\{(\lambda_j, \varphi_j)\}_{j \in \mathbb{N}^+}$ are eigenpairs of classical Laplacian operator $(-\Delta)$ (the infinitesimal generator of killed Brownian motion) with homogeneous Dirichlet boundary conditions on Ω .

*Corresponding author.

Email addresses: eyannyee@163.com (Yi Yang), huangjin12345@163.com (Jin Huang)

In this work, we will concentrate on the following nonlocal diffusion model

$$\begin{cases} \partial_t^\alpha u(\mathbf{x}, t) + \kappa_s(-\Delta + \gamma\mathbb{I})^s u(\mathbf{x}, t) = f(\mathbf{x}, t), & \mathbf{x} \in \Omega, \quad 0 < t \leq T, \\ u(\mathbf{x}, 0) = u_0(\mathbf{x}), & \mathbf{x} \in \Omega, \\ u(\mathbf{x}, t) = 0, & \mathbf{x} \in \partial\Omega, \quad 0 < t \leq T, \end{cases} \quad (2)$$

where $0 < s < 1$, $\gamma \geq 0$, $\kappa_s > 0$ the diffusion coefficient, \mathbb{I} the identity operator, and $\Omega \subset \mathbb{R}^d$ ($d = 1, 2, 3$) is a bounded open domain. The initial value $u_0(\mathbf{x})$ and source term $f(\mathbf{x}, t)$ are known, and the Djrbashian-Caputo fractional derivative of $u(\mathbf{x}, t)$ with respect to t is denoted by

$$\partial_t^\alpha u(\mathbf{x}, t) = \frac{1}{\Gamma(1-\alpha)} \int_0^t \frac{\partial u(\mathbf{x}, \tau)}{\partial \tau} \frac{d\tau}{(t-\tau)^\alpha}, \quad (3)$$

where $0 < \alpha < 1$, and $\Gamma(\cdot)$ is gamma function. Using the definition of spectral fractional Laplacian (SFL) in (1), we can derive the following SFL

$$(-\Delta + \gamma\mathbb{I})^s u(\mathbf{x}, t) = \sum_{j=1}^{\infty} (u, \varphi_j) (\lambda_j + \gamma)^s \varphi_j. \quad (4)$$

The time-space fractional diffusion problems have been widely studied, e.g., see [9, 11, 12] and the references therein. But all along, the nonlocal nature of time-space fractional derivatives brings us great challenges in numerical simulations. Hence this is critical to design efficiently and accurately fast algorithms for it. The primary goal of this work is to approximate SFL for (2) in spatial direction.

To the best of our current knowledge, various techniques have been established to deal with SFL: 1) Numerical methods based on Caffarelli-Silvestre extension, e.g., finite element method (FEM) [9, 13] and spectral method [14]; 2) From the viewpoint of Dunford-Taylor formula, some FEMs were proposed in [13, 15]; 3) Best uniform rational approximation [16–18]; 4) Numerical schemes combined with matrix transfer technique, for example, finite difference schemes [11, 12, 19, 20], FEMs [11, 21, 22], and also the spectral and spectral element methods reported in [23].

In this paper, we will be devoted to the fourth scheme, and then a critical point is that we need to solve fractional power of matrix. Different efficiently and accurately fast algorithms have been developed in [12, 24] because of special structure of matrix. However, some existing studies [11, 19–22, 25] only presented numerical approximation to fractional power of matrix, and iteration methods (e.g., conjugate gradient method) for matrix-vector multiplication are necessary.

Remarkably, we propose two fast and accurate solvers: linear FEM or fourth-order compact difference method (CDM) based on matrix transfer technique, which can efficiently approximate SFL for (2) in space. For the temporal discretization, a fast time stepping $L1$ scheme is presented. Our scheme can exactly compute the derived fractional power of matrix, and the matrix-vector multiplication is carried out by directly using discrete sine transform (DST) and inverse DST (iDST), which doesn't need to resort to any iteration method. It is noteworthy that the provided double fast algorithms can significantly reduce computation cost $\mathcal{O}(N^2\mathcal{N}^{d+1})$ to $\mathcal{O}(NQ\mathcal{N}^d \log \mathcal{N})$, \mathcal{N} is the maximum number of intervals in all spatial directions, and N the number of temporal intervals with $Q \ll N$.

Furthermore, it is tricky to address the convergence analysis of time-dependent problems in numerical methods combined with matrix transfer technique [11, 12]. To this end, we extend the means introduced in [20, 21] to time-space fractional diffusion problem (2) with inhomogeneous initial value and right hand side term. Then we can study the convergence analyses of full discrete scheme based on two types of spatial numerical methods. Particularly, compared with the usual regularity hypotheses in finite element analysis, we only require initial value part $\sum_{j=1}^{\infty} |(u_0(\cdot), \varphi_j)| (\lambda_j + \gamma)^{1+s} < \infty$ and source term part

$\sup_{0 \leq t \leq T} \sum_{j=1}^{\infty} |(f(\cdot, t), \varphi_j)| (\lambda_j + \gamma) < \infty$, then the corresponding optimal convergence estimate can be derived.

The remainder of this paper is organized as follows. In Section 2, linear FEM and fourth-order CDM combined with matrix transfer technique for SFL are proposed, and spatial semi-discrete scheme is derived. In Section 3, a fast time stepping $L1$ method is introduced. In addition, full discrete scheme based on two types of spatial numerical methods is developed, and the corresponding convergence analyses are discussed. Some numerical experiments are performed in Section 4. A summary is made in Section 5.

2. Spatial numerical method

In this section, we first introduce d -dimensional tensorial linear FEM and fourth-order CDM. Then we shall extend the numerical methods and matrix transform technique [11, 12, 19–22] to time-space fractional diffusion problem (2), and also derive the corresponding spatial semi-discrete scheme.

2.1. Tensorial numerical method

Throughout this paper, let $\Omega = \prod_{k=1}^d (a_k, b_k)$ be a bounded and open rectangular domain with $a_k < b_k$. Denote N_k as the number of meshgrids, take the spatial mesh size $h_k = \frac{b_k - a_k}{N_k}$, and define a finite dimensional space in the k -th spatial direction as

$$V_{h_k} = \text{span} \left\{ \phi_0^{(k)}, \phi_1^{(k)}, \dots, \phi_{N_k}^{(k)} \right\}, \quad k = 1, 2, \dots, d,$$

where $\phi_j^{(k)}$ is piecewise linear basis function for $j = 0, 1, \dots, N_k$. Then the d -dimensional tensorial finite element space V_h^d can be given by

$$V_h^d = V_{h_1} \otimes V_{h_2} \otimes \dots \otimes V_{h_d}, \quad d = 1, 2, 3,$$

where \otimes represents Kronecker product (or tensor product). In addition, we define a index set

$$\mathcal{T}_d = \{(i_1, i_2, \dots, i_d) \mid 1 \leq i_k \leq N_k - 1, k = 1, 2, \dots, d\}.$$

We now consider d -dimensional tensorial linear FEM or CDM for the auxiliary problem

$$\begin{cases} \kappa_s(-\Delta + \gamma \mathbb{I})u(\mathbf{x}) = f(\mathbf{x}), & \mathbf{x} \in \Omega, \\ u(\mathbf{x}) = 0, & \mathbf{x} \in \partial\Omega. \end{cases} \quad (5)$$

Thus, (5) can be formulated as the matrix-vector multiplication form

$$\kappa_s(M^{-1}S + \gamma I)\mathbf{u} = K\mathbf{b},$$

where I , S , M and \mathbf{b} denote identity matrix, stiffness matrix, mass matrix and right hand side vector, respectively. Here, we let

$$K = K_1 \otimes \dots \otimes K_{k-1} \otimes K_k \otimes K_{k+1} \otimes \dots \otimes K_d,$$

with $K_k = I_k$ in FEM if $f \in V_h^d$ or in CDM; while $K_k = M_k^{-1}$ in FEM if $f \notin V_h^d$, where I_k and M_k will be defined below. Significantly, we have also the following

$$S = \sum_{k=1}^d (M_1 \otimes \dots \otimes M_{k-1} \otimes A_k \otimes M_{k+1} \otimes \dots \otimes M_d),$$

as well as

$$M = M_1 \otimes \cdots \otimes M_{k-1} \otimes M_k \otimes M_{k+1} \otimes \cdots \otimes M_d, \quad I = I_1 \otimes \cdots \otimes I_{k-1} \otimes I_k \otimes I_{k+1} \otimes \cdots \otimes I_d,$$

where

$$A_k = \begin{pmatrix} a & b & 0 & 0 & \cdots & 0 \\ b & a & b & 0 & \cdots & 0 \\ \vdots & \ddots & \ddots & \ddots & \ddots & \vdots \\ 0 & \cdots & 0 & b & a & b \\ 0 & \cdots & 0 & 0 & b & a \end{pmatrix}, \quad \text{and} \quad M_k = \begin{pmatrix} c & d & 0 & 0 & \cdots & 0 \\ d & c & d & 0 & \cdots & 0 \\ \vdots & \ddots & \ddots & \ddots & \ddots & \vdots \\ 0 & \cdots & 0 & d & c & d \\ 0 & \cdots & 0 & 0 & d & c \end{pmatrix},$$

where $a = \frac{2}{h_k}$ or $\frac{2}{h_k^2}$, $b = \frac{-1}{h_k}$ or $\frac{-1}{h_k^2}$, $c = \frac{4h_k}{6}$ or $\frac{10}{12}$, and $d = \frac{h_k}{6}$ or $\frac{1}{12}$ if A_k and M_k are in FEM or CDM, respectively. In addition, I_k is $(N_k - 1)$ by $(N_k - 1)$ identity matrix. It is noteworthy that $(N_k - 1)$ by $(N_k - 1)$ matrices A_k and M_k are symmetric and tridiagonal, their eigenvalues can be expressed as

$$\lambda_i^{(s_k)} = a - 2|b| \cos\left(\frac{i\pi}{N_k}\right), \quad \text{and} \quad \lambda_i^{(m_k)} = c + 2|d| \cos\left(\frac{i\pi}{N_k}\right),$$

respectively, and the eigenvectors of both of them are $(P_k)_{ij} = \sin\left(\frac{ij\pi}{N_k}\right)$ for $i, j = 1, 2, \dots, N_k - 1$. Therefore, A_k and M_k can be, respectively, diagonalized as

$$A_k = P_k \Lambda_{s_k} P_k^{-1}, \quad \text{and} \quad M_k = P_k \Lambda_{m_k} P_k^{-1}, \quad (6)$$

where the diagonal matrices

$$\Lambda_{s_k} = \text{diag}\left(\lambda_1^{(s_k)}, \lambda_2^{(s_k)}, \dots, \lambda_{N_k-1}^{(s_k)}\right), \quad \text{and} \quad \Lambda_{m_k} = \text{diag}\left(\lambda_1^{(m_k)}, \lambda_2^{(m_k)}, \dots, \lambda_{N_k-1}^{(m_k)}\right).$$

Below, we will consider the discretization of time-space fractional diffusion problem (2).

2.2. Spatial semi-discretization

In this part, we will extend the two types of numerical methods combined with matrix transform technique to time-space fractional diffusion problem (2), and derive its spatial semi-discrete scheme.

We now study the spatial semi-discretization of diffusion problem (2). Based on the means developed in the preceding subsection, we have the following matrix-vector multiplication form

$$(\partial_t^\alpha + \kappa_s(M^{-1}S + \gamma I)^s) \mathbf{u}(t) = K\mathbf{b}(t). \quad (7)$$

The next core goal is to deal with the s fractional power of $(M^{-1}S + \gamma I)$ in (7). Remarkably, it can be calculated accurately and fastly.

In terms of the inverse properties of Kronecker products and its matrix multiplication, we have

$$\begin{aligned} M^{-1}S &= \sum_{k=1}^d ((M_1^{-1}M_1) \otimes \cdots \otimes (M_{k-1}^{-1}M_{k-1}) \otimes (M_k^{-1}A_k) \otimes (M_{k+1}^{-1}M_{k+1}) \otimes \cdots \otimes (M_d^{-1}M_d)) \\ &= \sum_{k=1}^d (I_1 \otimes \cdots \otimes I_{k-1} \otimes (M_k^{-1}A_k) \otimes I_{k+1} \otimes \cdots \otimes I_d). \end{aligned}$$

Therefore, we can obtain

$$\begin{aligned}
(M^{-1}S + \gamma I) &= \sum_{k=1}^d (I_1 \otimes \cdots \otimes I_{k-1} \otimes (M_k^{-1}A_k) \otimes I_{k+1} \otimes \cdots \otimes I_d \\
&\quad + \frac{\gamma}{d} I_1 \otimes \cdots \otimes I_{k-1} \otimes I_k \otimes I_{k+1} \otimes \cdots \otimes I_d) \\
&= \sum_{k=1}^d (I_1 \otimes \cdots \otimes I_{k-1} \otimes (M_k^{-1}A_k + \frac{\gamma}{d}I_k) \otimes I_{k+1} \otimes \cdots \otimes I_d).
\end{aligned}$$

Moreover, from the diagonalization (6), we denote T_k as

$$T_k := (M_k^{-1}A_k + \frac{\gamma}{d}I_k) = P_k \Lambda_k P_k^{-1},$$

where $\Lambda_k := \text{diag}(\lambda_1^{(k)}, \lambda_2^{(k)}, \dots, \lambda_{N_k-1}^{(k)})$ with $\lambda_i^{(k)} = \left(\frac{\lambda_i^{(s_k)}}{\lambda_i^{(m_k)}} + \frac{\gamma}{d} \right)$ for $i = 1, 2, \dots, N_k - 1$. Then using generalized multinomial theorem yields

$$\begin{aligned}
(M^{-1}S + \gamma I)^s &= \left(\sum_{k=1}^d (I_1 \otimes \cdots \otimes I_{k-1} \otimes T_k \otimes I_{k+1} \otimes \cdots \otimes I_d) \right)^s \\
&= \sum_{n_{d-1}=0}^{\infty} \sum_{n_{d-2}=0}^{n_{d-1}} \cdots \sum_{n_1=0}^{n_2} \binom{s}{n_{d-1}} \binom{n_{d-1}}{n_{d-2}} \cdots \binom{n_2}{n_1} (I_1 \otimes \cdots \otimes I_{d-1} \otimes T_d)^{s-n_{d-1}} \\
&\quad \times (I_1 \otimes \cdots \otimes I_{d-2} \otimes T_{d-1} \otimes I_d)^{n_{d-1}-n_{d-2}} \cdots (T_1 \otimes I_2 \otimes \cdots \otimes I_d)^{n_1} \\
&= \sum_{n_{d-1}=0}^{\infty} \sum_{n_{d-2}=0}^{\infty} \cdots \sum_{n_1=0}^{\infty} \binom{s}{n_1, n_2, \dots, n_{d-1}} (T_1 \otimes I_2 \otimes \cdots \otimes I_d)^{n_1} \cdots \\
&\quad \times (I_1 \otimes \cdots \otimes I_{d-2} \otimes T_{d-1} \otimes I_d)^{n_{d-1}} (I_1 \otimes \cdots \otimes I_{d-1} \otimes T_d)^{s-n_1-\cdots-n_{d-1}}, \tag{8}
\end{aligned}$$

where the generalized multinomial coefficient

$$\binom{s}{n_1, n_2, \dots, n_{d-1}} := \binom{s}{n_1 + n_2 + \cdots + n_{d-1}} \binom{n_1 + n_2 + \cdots + n_{d-1}}{n_1 + n_2 + \cdots + n_{d-2}} \cdots \binom{n_1 + n_2}{n_1}.$$

In what follows, the treatment means of (8) will be coincidence with [12], so we directly have

$$(M^{-1}S + \gamma I)^s \mathbf{u}(t) = P_1 \otimes \cdots \otimes P_{d-1} P_d \odot (H_d \odot (P_1^{-1} \otimes \cdots \otimes P_{d-1}^{-1} \otimes U(t))), \tag{9}$$

where H_d is a d -dimensional array with the (i_1, i_2, \dots, i_d) -th entry

$$(H_d)_{i_1, i_2, \dots, i_d} = \left(\sum_{k=1}^d \lambda_{i_k}^{(k)} \right)^s, \quad (i_1, i_2, \dots, i_d) \in \mathcal{T}_d, \tag{10}$$

the operator \odot represents Hadamard matrix product, also $U(t) = \{\mathbf{u}_{i_1, i_2, \dots, i_d}(t)\}_{(N_1-1) \times \cdots \times (N_d-1)}$ is a d -dimensional array. Furthermore, the notation \otimes_k is defined by

$$(W \otimes_k R)_{i_1, i_2, \dots, i_d} := \sum_{j=1}^{N_k-1} W_{i_k, j} R_{i_1, \dots, i_{k-1}, j, i_{k+1}, \dots, i_d},$$

where W is $(N_k - 1)$ by $(N_k - 1)$ matrix, and R denotes a d -dimensional array.

We now consider the computation of right hand side term. For different matrices K , we have

$$\begin{aligned} K\mathbf{b}(t) &= (K_1 \otimes \cdots \otimes K_{k-1} \otimes K_k \otimes K_{k+1} \otimes \cdots \otimes K_d) \mathbf{b}(t) \\ &= P_1 \otimes_1 \cdots \otimes_{d-1} P_d \otimes_d (V_d \odot (P_1^{-1} \otimes_1 \cdots \otimes_{d-1} P_d^{-1} \otimes_d F(t))), \end{aligned} \quad (11)$$

where V_d is a d -dimensional array with the (i_1, i_2, \dots, i_d) -th entry

$$(V_d)_{i_1, i_2, \dots, i_d} = \prod_{k=1}^d \bar{\lambda}_{i_k}^{(k)}, \quad (i_1, i_2, \dots, i_d) \in \mathcal{T}_d, \quad (12)$$

where $\bar{\lambda}_{i_k}^{(k)}$ is the i_k -th eigenvalue of K_k , and $F(t) = \{\mathbf{b}_{i_1, i_2, \dots, i_d}(t)\}_{(N_1-1) \times \cdots \times (N_d-1)}$ is also a d -dimensional array with the entry

$$\mathbf{b}_{i_1, i_2, \dots, i_d}(t) = f(x_{1_{i_1}}, x_{2_{i_2}}, \dots, x_{d_{i_d}}, t), \quad \text{or } \mathbf{b}_{i_1, i_2, \dots, i_d}(t) = \left(f(\cdot, t), \prod_{k=1}^d \phi_{i_k}^{(k)} \right).$$

In addition, it follows from [12, 26, 27] that

$$P_1 \otimes_1 \cdots \otimes_{d-1} P_d \otimes_d R = \mathcal{D}_d(R), \quad \text{and } P_1^{-1} \otimes_1 \cdots \otimes_{d-1} P_d^{-1} \otimes_d R = \mathcal{D}_d^{-1}(R), \quad (13)$$

where \mathcal{D}_d and \mathcal{D}_d^{-1} represent d -dimensional DST and iDST, respectively, and R is a d -dimensional array.

Hence, using (9), (11) and (13), the semi-discrete scheme of problem (2) can be written as

$$\partial_t^\alpha U(t) + \mathcal{D}_d(\kappa_s H_d \odot \mathcal{D}_d^{-1}(U(t))) = \mathcal{D}_d(V_d \odot \mathcal{D}_d^{-1}(F(t))), \quad t \in (0, T]. \quad (14)$$

Remark 1. If we just consider the time-independent fractional diffusion equation (5), then its numerical solution can be expressed as

$$U = \mathcal{D}_d(L_d \odot (V_d \odot \mathcal{D}_d^{-1}(F))),$$

where $F = \{\mathbf{b}_{i_1, i_2, \dots, i_d}\}_{(N_1-1) \times \cdots \times (N_d-1)}$ is a d -dimensional array, and L_d is defined as

$$(L_d)_{i_1, i_2, \dots, i_d} = 1/(\kappa_s H_d)_{i_1, i_2, \dots, i_d}, \quad (i_1, i_2, \dots, i_d) \in \mathcal{T}_d.$$

In particular, if $f(\mathbf{x}) \in V_h^d \subset L^2(\Omega)$, then we have also

$$U = \mathcal{D}_d(L_d \odot \mathcal{D}_d^{-1}(F)),$$

where the d -dimensional array $F = \left\{ f(x_{1_{i_1}}, x_{2_{i_2}}, \dots, x_{d_{i_d}}) \right\}_{(N_1-1) \times \cdots \times (N_d-1)}$.

Remark 2. If $M = I$ in the CDM, then (7) or (14) reduces to the second-order central finite difference semi-discrete scheme [12] for (2) in space.

In the next section, we will address the implementation and convergence analysis of full discrete scheme which is based on a fast time stepping $L1$ method [28–31] in time.

3. Implementation and analysis of full discrete scheme

Though a fast Fourier algorithm has been presented in space, it is still difficult for us to numerically simulate the high dimensional time-space fractional diffusion problem (2) in temporal direction. Hence, it is quietly critical to choose a fast and low memory discrete technique for Caputo derivative (3).

In this part, we first introduce a fast time stepping $L1$ scheme for time discretization, and induce the full discrete scheme of (2). In the end, we also give the corresponding convergence analysis.

3.1. Implementation of fast time stepping

Let N be the number of elements in temporal direction, and \mathcal{I}^1 be linear Lagrange interpolation operator. Given $t_n = n\Delta t$ with uniform time step size $\Delta t = TN^{-1}$ for $n = 0, 1, \dots, N$, we take $t = t_n$ such that

$$\partial_t^\alpha \mathbf{u}(t_n) = \frac{1}{\Gamma(1-\alpha)} \int_0^{t_n} \frac{\partial \mathbf{u}(\tau)}{\partial \tau} (t_n - \tau)^{-\alpha} d\tau, \quad n = 1, 2, \dots, N.$$

Interpolating linearly $\mathbf{u}(\tau)$ with respect to variable τ , and using the integration by parts on interval $[0, t_{n-1}]$, we have

$$\begin{aligned} \partial_t^\alpha \mathbf{u}(t_n) &\approx \frac{1}{\Gamma(1-\alpha)} \int_{t_{n-1}}^{t_n} \frac{\partial \mathcal{I}^1 \mathbf{u}(\tau)}{\partial \tau} (t_n - \tau)^{-\alpha} d\tau + \frac{1}{\Gamma(1-\alpha)} \int_0^{t_{n-1}} \frac{\partial \mathcal{I}^1 \mathbf{u}(\tau)}{\partial \tau} (t_n - \tau)^{-\alpha} d\tau \\ &= \underbrace{\frac{\mathbf{u}(t_n) - \alpha \mathbf{u}(t_{n-1}) - (1-\alpha)\mathbf{u}(t_0)n^{-\alpha}}{\Delta t^\alpha \Gamma(2-\alpha)}}_{L^\alpha \mathbf{u}(t_n)} + \underbrace{\frac{1}{\Gamma(-\alpha)} \int_0^{t_{n-1}} \frac{\mathcal{I}^1 \mathbf{u}(\tau)}{(t_n - \tau)^{1+\alpha}} d\tau}_{H^\alpha \mathbf{u}(t_n)}. \end{aligned} \quad (15)$$

where $L^\alpha \mathbf{u}(t_n)$ is local part, and $H^\alpha \mathbf{u}(t_n)$ is history part.

In order to develop a fast time stepping $L1$ method, we now introduce a sum of exponentials to approximate kernel function [28–31]:

$$\frac{t^{-\alpha-1}}{\Gamma(-\alpha)} = \sum_{j=1}^Q w_j e^{\xi_j t} + O(\varepsilon t^{-\alpha-1}), \quad t \in [t_1, T],$$

where $\varepsilon > 0$ is the precision, $Q > 1$ is a positive integer, and the nodes ξ_j and weights w_j are known. Hence, we have

$$H^\alpha \mathbf{u}(t_n) = \sum_{j=1}^Q w_j e^{\xi_j \Delta t} Y_j(t_{n-1}) + O(\varepsilon \Delta t), \quad (16)$$

where $Y_j(t) = \int_0^t e^{\xi_j(t-\tau)} \mathcal{I}^1 \mathbf{u}(\tau) d\tau$ satisfies

$$(Y_j)'(t) = \xi_j Y_j(t) + \mathcal{I}^1 \mathbf{u}(t), \quad \text{with } Y_j(0) = 0,$$

which can be exactly solved by

$$Y_j(t_i) = \kappa_1 Y_j(t_{i-1}) + \kappa_2 \mathbf{u}(t_{i-1}) + \kappa_3 \mathbf{u}(t_i), \quad \text{with } Y_j(t_0) = 0, \quad i \geq 1,$$

where $\kappa_1 = e^z$, $\kappa_2 = \frac{1}{\xi_j} (e^z - 1 - \frac{e^z - z - 1}{z})$, $\kappa_3 = \frac{1}{\xi_j} \frac{e^z - z - 1}{z}$ and $z = \xi_j \Delta t$.

In this work, we assume that the fast time stepping $L1$ method is based on a trapezoidal rule on the real line [30]. From (15) and (16), $\partial_t^\alpha \mathbf{u}(t)$ at $t = t_n$ can be approximated by

$$\partial_t^\alpha \mathbf{u}(t_n) = \bar{\partial}_t^\alpha \mathbf{u}(t_n) + r^n, \quad (17)$$

where r^n is truncation error, and the discrete differential operator $\bar{\partial}_t^\alpha$ is defined by

$$\bar{\partial}_t^\alpha \mathbf{u}(t_n) := \frac{\mathbf{u}(t_n) - \alpha \mathbf{u}(t_{n-1}) - (1-\alpha)n^{-\alpha} \mathbf{u}(t_0)}{\tau} + \sum_{j=1}^Q w_j e^{\xi_j \Delta t} Y_j(t_{n-1}), \quad n = 1, 2, \dots, N,$$

where $\tau = \Delta t^\alpha \Gamma(2-\alpha)$, and the above sum term will vanish for $n \leq 1$.

We note from [28] that the following lemma can be obtained.

Lemma 3.1. *If $\mathbf{u}(t) \in C^2[0, T]$, then the truncation error r^n of the fast time stepping L1 scheme can be also bounded by*

$$|r^n| \leq C \max_{0 \leq t \leq T} |\mathbf{u}_{tt}(t)| \Delta t^{2-\alpha} + C_1(n-1)\varepsilon\Delta t, \quad n = 1, 2, \dots, N,$$

where C and C_1 are two positive constants.

From (7) and (17), we have

$$(1 + \tau\kappa_s(M^{-1}S + \gamma I)^s) \mathbf{u}(t_n) = \mathbf{g}(t_n) + \tau K \mathbf{b}(t_n) - r^n, \quad (18)$$

where $\mathbf{g}(t_n)$ is defined by

$$\mathbf{g}(t_n) := \alpha \mathbf{u}(t_{n-1}) + (1 - \alpha)n^{-\alpha} \mathbf{u}(t_0) - \tau \sum_{j=1}^Q w_j e^{\xi_j \Delta t} Y_j(t_{n-1}).$$

Let \mathbf{u}^n be an approximation to $\mathbf{u}(t_n)$, and $\mathbf{g}_{i_1, i_2, \dots, i_d}^n$ be an approximation to $\mathbf{g}_{i_1, i_2, \dots, i_d}(t_n)$. From (9), (11), (13) and (18), we can obtain the following fully discrete scheme

$$\mathcal{D}_d((E_d + \tau\kappa_s H_d) \odot \mathcal{D}_d^{-1}(U^n)) = G_d^n + \tau \mathcal{D}_d(V_d \odot \mathcal{D}_d^{-1}(F^n)), \quad (19)$$

where E_d is a d -dimensional array with entry $(E_d)_{i_1, i_2, \dots, i_d} = 1$ for $(i_1, i_2, \dots, i_d) \in \mathcal{T}_d$, H_d and V_d can be seen in (10) and (12). In addition, $U^n = \{\mathbf{u}_{i_1, i_2, \dots, i_d}^n\}_{(N_1-1) \times \dots \times (N_d-1)}$, $F^n = \{\mathbf{b}_{i_1, i_2, \dots, i_d}(t_n)\}_{(N_1-1) \times \dots \times (N_d-1)}$ and $G_d^n = \{\mathbf{g}_{i_1, i_2, \dots, i_d}^n\}_{(N_1-1) \times \dots \times (N_d-1)}$ are three d -dimensional arrays for $n = 0, 1, 2, \dots, N$.

Finally, taking successively iDST and DST on both sides of (19), we have

$$U^n = \mathcal{D}_d(L_d \odot (G_d^n + \tau(V_d \odot \mathcal{D}_d^{-1}(F^n))))), \quad n = 1, 2, \dots, N, \quad (20)$$

which is based on double fast algorithms in time and space, where L_d is a d -dimensional array with entry

$$(L_d)_{i_1, i_2, \dots, i_d} := \frac{1}{1 + \tau\kappa_s(H_d)_{i_1, i_2, \dots, i_d}}, \quad (i_1, i_2, \dots, i_d) \in \mathcal{T}_d.$$

In general, the numerical solutions of full discrete scheme based on L1 method possess strong history dependence, that is, the solutions of the current time step t_n will depend on the solutions of all previous time steps t_k for $k = 0, 1, \dots, n-1$. However, in the proposed scheme (19), we can clearly note that the solution of the current time step t_n just depends on the solutions of time steps t_{n-1} , t_{n-2} and t_0 . For spatial discretization, the nonlocality is reflected in that discrete matrix is dense. Remarkably, we can exactly compute the matrix fractional power, and don't need to resort to iteration method in matrix-vector multiplication by directly using DST and iDST.

Moreover, the presented double fast algorithms can efficiently overcome the nonlocality in our numerical simulations, and it can significantly reduce the computational cost from $\mathcal{O}(N^2 \mathcal{N}^{d+1})$ by a direct matrix-vector multiplication to $\mathcal{O}(NQ \mathcal{N}^d \log \mathcal{N})$ with $\mathcal{N} = \max_{1 \leq k \leq d} N_k$ and $Q \ll N$.

Remark 3. *As $\alpha \rightarrow 1^-$, the solution in (20) reduces to*

$$U^n = \mathcal{D}_d(L_d \odot (\mathcal{D}_d^{-1}(U^{n-1}) + \tau(V_d \odot \mathcal{D}_d^{-1}(F^n))))),$$

where $\tau = \Delta t$, i.e., a standard first-order backward difference scheme is used in the temporal direction.

3.2. Convergence analysis

In this subsection, we are devoted to studying the convergence analysis of full discrete scheme (19). To this end, we first introduce Mittag-Leffler function, and then recall some basic function spaces. Finally, we establish optimal error estimates of full discrete scheme (19).

To derive the analytical solution of (2), it is essential to introduce the Mittag-Leffler function

$$E_{\alpha,\beta}(z) = \sum_{k=0}^{\infty} \frac{z^k}{\Gamma(k\alpha + \beta)}, \quad z \in \mathbb{C},$$

where $\beta \in \mathbb{R}$ and $0 < \alpha < 1$. Now we give the Fourier expansions of the data u_0 , f and u . Namely, let $u(t) := \sum_{j=1}^{\infty} (u(\cdot, t), \varphi_j) \varphi_j$, $f(t) := \sum_{j=1}^{\infty} (f(\cdot, t), \varphi_j) \varphi_j$ and $u_0 := \sum_{j=1}^{\infty} (u_0(\cdot), \varphi_j) \varphi_j$.

Hence, using separation of variable and resorting to the Mittag-Leffler function $E_{\alpha,\beta}$, the solution u of problem (2) can be represented as

$$u(t) = E(t)u_0 + \int_0^t \bar{E}(t-\tau)f(\tau)d\tau, \quad (21)$$

where the solution operator

$$E(t)u_0 = \sum_{j=1}^{\infty} E_{\alpha,1}(-\kappa_s(\lambda_j + \gamma)^s t^\alpha) (u_0, \varphi_j) \varphi_j,$$

and the solution operator \bar{E} for $\chi \in L^2(\Omega)$ is defined by

$$\bar{E}(t)\chi = \sum_{j=1}^{\infty} t^{\alpha-1} E_{\alpha,\alpha}(-\kappa_s(\lambda_j + \gamma)^s t^\alpha) (\chi, \varphi_j) \varphi_j.$$

Before studying the error analysis of full discrete scheme, we also need to give two important properties on the function $E_{\alpha,\beta}$, which can be seen in [32].

Lemma 3.2. *Let $0 < \alpha < 1$, $\beta \in \mathbb{R}$, and $\frac{\alpha\pi}{2} < \mu < \min\{\pi, \pi\alpha\}$. Then there exists constant $C = C(\alpha, \beta, \mu) > 0$ such that*

$$E_{\alpha,\beta}(z) \leq \frac{C}{1+|z|}, \quad \mu \leq |\arg(z)| \leq \pi, \quad z \in \mathbb{C}.$$

Lemma 3.3. *Suppose that $\eta > 0$ and $\mu > 0$. Then we have*

$$\int_0^\eta \tau^{\alpha-1} E_{\alpha,\alpha}(-\mu\tau^\alpha) d\tau = -\frac{1}{\mu} \int_0^\eta \frac{d}{d\tau} E_{\alpha,1}(-\mu\tau^\alpha) d\tau = \frac{1}{\mu} (1 - E_{\alpha,1}(-\mu\eta^\alpha)).$$

Next, we recall some basic function spaces. The square integrable function space is $L^2(\Omega)$ with norm $\|\cdot\|$ and inner product (\cdot, \cdot) . For $s \geq -1$, $\dot{H}^s(\Omega) \subset H^{-1}(\Omega)$ denotes a Hilbert space equipped with the norm

$$\|v\|_{\dot{H}^s(\Omega)}^2 = \sum_{j=1}^{\infty} (\lambda_j + \gamma)^s (v, \varphi_j)^2.$$

Given a Banach space X and arbitrary $p \geq 1$, we can define the space

$$L^p(0, T; X) = \{v(t) \in X \text{ for a.e. } t \in (0, T) \text{ and } \|v\|_{L^p(0, T; X)} < \infty\},$$

and its norm $\|\cdot\|_{L^p(0,T;X)}$ is induced by

$$\|v\|_{L^p(0,T;X)} = \begin{cases} \left(\int_0^T \|v(t)\|_X^p dt \right)^{1/p}, & p \in [1, \infty), \\ \operatorname{ess\,sup}_{t \in (0,T)} \|v(t)\|_X, & p = \infty. \end{cases}$$

Furthermore, $(-\Delta + \gamma\mathbb{I})$ is a positive self-adjoint operator. Then, for all $u \in \dot{H}^{2s}(\Omega)$ and v belonging to a Hilbert space, by using Balakrishnan's representation, we have

$$((-\Delta + \gamma\mathbb{I})^s u, v) = \frac{\sin(\pi s)}{\pi} \int_0^\infty (z^{s-1}(-\Delta + \gamma\mathbb{I})(z\mathbb{I} + (-\Delta + \gamma\mathbb{I}))^{-1}u, v) dz. \quad (22)$$

Introducing a elliptic projection $P_h : H_0^k(\Omega) \rightarrow V_h^d \subset H_0^k(\Omega)$ ($k = 2$) such that for $u \in H_0^k(\Omega)$, we have

$$((-\Delta + \gamma\mathbb{I})P_h u, v_h) = ((-\Delta + \gamma\mathbb{I})u, v_h), \quad \forall v_h \in V_h^d.$$

Hence the following projection estimate holds

$$\|v - P_h v\| \leq Ch^k \|v\|_k, \quad \forall v \in H_0^k(\Omega), \quad k = 2, \quad (23)$$

where h is spatial mesh size. Besides, we also define a linear bijection $\pi_h : V_h^d \rightarrow \mathbb{R}^m$, with $\pi_h(u_h) = \mathbf{u}$, here \mathbf{u} is solution vector, and $m = \prod_{k=1}^d (N_k - 1)$ is the degrees of freedom.

Though the proposed fast finite element scheme is based on bilinear interpolation, the following discussions can also be extended to high order interpolation. Therefore, we first study the error analysis of full discrete scheme in FEM, and it is also valid when $k \in \mathbb{N}^+$ and $k \geq 2$.

Lemma 3.4. *Let $\Delta_h = \pi_h^{-1}M^{-1}(S+M)\pi_h$ represent discrete Laplacian operator. The following estimation holds*

$$|((-\Delta + \gamma\mathbb{I})^s \varphi_j - (-\Delta_h + \gamma\mathbb{I})^s P_h \varphi_j, v_h)| \leq Ch^k (\lambda_j + \gamma)^s \|\varphi_j\|_k \|v_h\|, \quad v_h \in V_h^d,$$

where C is a positive constant.

Using formulation (22) and a similar means in [21], the proof of Lemma 3.4 can be obtained. In that paper, authors only discussed error analysis in space fractional diffusion problem with first-order time derivative and homogeneous right hand side term.

Below, we will extend the technique developed in [21] to time-space fractional diffusion problem with inhomogenous initial value and right hand side term. For simplicity, we temporarily denote $u_j(t) := (u(\cdot, t), \varphi_j)$, $f_j(t) := (f(\cdot, t), \varphi_j)$ and $u_{0j} := (u_0(\cdot), \varphi_j)$.

Theorem 3.1. *Suppose that $\nu_0 = \sum_{j=1}^\infty |u_{0j}| (\lambda_j + \gamma)^{\frac{k}{2} + s} < \infty$ and $\nu_1 = \sup_{0 \leq t \leq T} \sum_{j=1}^\infty (\lambda_j + \gamma)^{\frac{k}{2}} |f_j(t)| < \infty$. If $u(t)$ in (21) is the solution of (2), then we have*

$$|((-\Delta + \gamma\mathbb{I})^s u(t) - (-\Delta_h + \gamma\mathbb{I})^s P_h u(t), v_h)| \leq C (\nu_0 + \nu_1) h^k \|v_h\|, \quad v_h \in V_h^d,$$

for $t > 0$, where C is a positive constant.

Proof. By the boundness of $E_{\alpha,\beta}$ in Lemma 3.2 and the property in Lemma 3.3, we have

$$\begin{aligned} |u_j(t)| &= \left| u_{0j} E_{\alpha,1}(-\kappa_s (\lambda_j + \gamma)^s t^\alpha) + \int_0^t (t-\tau)^{\alpha-1} E_{\alpha,\alpha}(-\kappa_s (\lambda_j + \gamma)^s (t-\tau)^\alpha) f_j(\tau) d\tau \right| \\ &\leq |u_{0j}| \frac{C_1}{1 + \kappa_s (\lambda_j + \gamma)^s t^\alpha} + \sup_{0 \leq \tau \leq T} |f_j(\tau)| \left| \int_0^t (t-\tau)^{\alpha-1} E_{\alpha,\alpha}(-\kappa_s (\lambda_j + \gamma)^s (t-\tau)^\alpha) d\tau \right| \\ &\leq C_1 |u_{0j}| + \frac{C_2}{(\lambda_j + \gamma)^s} \sup_{0 \leq \tau \leq T} |f_j(\tau)|, \quad \forall t > 0. \end{aligned} \quad (24)$$

In addition, the $H^k(\Omega)$ norm of $\{\varphi_j\}_{j=1}^\infty$ satisfy the following growth condition:

$$\|\varphi_j\|_k \leq C\lambda_j^{\frac{k}{2}} \leq C(\lambda_j + \gamma)^{\frac{k}{2}}. \quad (25)$$

Hence, using (24), (25) and Lemma 3.4, we can derive the estimate

$$\begin{aligned} |(((-\Delta + \gamma\mathbb{I})^s - (-\Delta_h + \gamma\mathbb{I})^s P_h) u(t), v_h)| &= \left| \left(\sum_{j=1}^{\infty} u_j(t) ((-\Delta + \gamma\mathbb{I})^s - (-\Delta_h + \gamma\mathbb{I})^s P_h) \varphi_j, v_h \right) \right| \\ &\leq \sum_{j=1}^{\infty} |(u_j(t) ((-\Delta + \gamma\mathbb{I})^s - (-\Delta_h + \gamma\mathbb{I})^s P_h) \varphi_j, v_h)| \\ &\leq Ch^k \|v_h\| \sum_{j=1}^{\infty} \|\varphi_j\|_k |u_j(t)| (\lambda_j + \gamma)^s \leq Ch^k \|v_h\| \sum_{j=1}^{\infty} |u_j(t)| (\lambda_j + \gamma)^{\frac{k}{2}+s} \\ &\leq Ch^k \|v_h\| \left(\sum_{j=1}^{\infty} |u_{0j}| (\lambda_j + \gamma)^{\frac{k}{2}+s} + \sup_{0 \leq \tau \leq T} \sum_{j=1}^{\infty} (\lambda_j + \gamma)^{\frac{k}{2}} |f_j(\tau)| \right), \quad \forall v_h \in V_h^d. \end{aligned}$$

This completes the proof. \square

Theorem 3.2. *Under the assumptions of Lemma 3.1, Lemma 3.4, Theorem 3.1 and $P_h u^0 = u_h^0$, the full discrete scheme (19) is $\mathcal{O}(\Delta t^{2-\alpha} + h^k + \varepsilon)$ optimal convergence, ε is small sufficiently enough to be ignored.*

Proof. For simplicity of analysis, we first derive a full discrete scheme. Find $u_h^n \in V_h^d$ such that

$$(\bar{\partial}_t^\alpha u_h^n, v_h) + \kappa_s ((-\Delta_h + \gamma\mathbb{I})^s u_h^n, v_h) = (f, v_h), \quad \forall v_h \in V_h^d. \quad (26)$$

Hence $P_h u^n$ with $u^n := u(t_n)$ also satisfies

$$(\bar{\partial}_t^\alpha P_h u^n, v_h) + \kappa_s ((-\Delta_h + \gamma\mathbb{I})^s P_h u^n, v_h) = (f, v_h), \quad \forall v_h \in V_h^d. \quad (27)$$

Making use of (27) and equality $\kappa_s ((-\Delta + \gamma\mathbb{I})^s u^n, v_h) = (f^n - \partial_t^\alpha u^n, v_h)$ with $f^n := f(\cdot, t_n)$, we have

$$\begin{aligned} (\bar{\partial}_t^\alpha P_h u^n, v_h) + \kappa_s ((-\Delta_h + \gamma\mathbb{I})^s P_h u^n, v_h) \\ = ((\bar{\partial}_t^\alpha - \partial_t^\alpha) u^n, v_h) + (f^n, v_h) + (\bar{\partial}_t^\alpha (P_h - \mathbb{I}) u^n, v_h) \\ + \kappa_s (((-\Delta_h + \gamma\mathbb{I})^s P_h - (-\Delta + \gamma\mathbb{I})^s) u^n, v_h). \end{aligned} \quad (28)$$

From Lemma 3.1, we can estimate

$$\|\bar{\partial}_t^\alpha u^n - \partial_t^\alpha u^n\| = \|r^n\| \leq C\Delta t^{2-\alpha} \max_{0 \leq \tau \leq t_n} \|u_{tt}(\cdot, \tau)\| + C_1(n-1)\varepsilon\Delta t. \quad (29)$$

In addition, using formulation (23) and Lemma 3.1 easily results in

$$\|\bar{\partial}_t^\alpha (P_h - \mathbb{I}) u^n\| \leq h^k \|\partial_t^\alpha u^n\|_{L^\infty(t_n, t_{n+1}; H^k(\Omega))} + \mathcal{O}(\Delta t^{2-\alpha} h^k + \varepsilon \Delta t h^k). \quad (30)$$

Now, denoting $\rho^n = P_h u^n - u_h^n$, and subtracting (26) from (28), we have

$$\begin{aligned} (\bar{\partial}_t^\alpha \rho^n, v_h) + \kappa_s ((-\Delta_h + \gamma\mathbb{I})^s \rho^n, v_h) &= ((\bar{\partial}_t^\alpha - \partial_t^\alpha) u^n, v_h) + (\bar{\partial}_t^\alpha (P_h - \mathbb{I}) u^n, v_h) \\ &\quad + \kappa_s (((-\Delta_h + \gamma\mathbb{I})^s P_h - (-\Delta + \gamma\mathbb{I})^s) u^n, v_h). \end{aligned}$$

Taking $v_h = \rho^n$ in the above quality, and using the positivity of $(-\Delta_h + \gamma\mathbb{I})^s$ leads to

$$\begin{aligned} \|\rho^n\| &\leq \tau \left\| (\bar{\partial}_t^\alpha - \partial_t^\alpha) u^n \right\| + \tau \left\| \bar{\partial}_t^\alpha (P_h - \mathbb{I}) u^n \right\| + \tau \kappa_s \left\| ((-\Delta_h + \gamma\mathbb{I})^s P_h - (-\Delta + \gamma\mathbb{I})^s) u^n \right\| \\ &\quad + \tau \left\| \sum_{j=1}^Q w_j e^{\xi_j \Delta t} Y_j(t_{n-1}) \right\| + \alpha \|\rho^{n-1}\| + (1 - \alpha) n^{-\alpha} \|\rho^0\|, \end{aligned} \quad (31)$$

where $Y_j(t_{n-1}) = k_1 Y_j(t_{n-2}) + k_2 \mathcal{I}^1 \rho^{n-2} + k_3 \mathcal{I}^1 \rho^{n-1}$. From (29)-(31) and Theorem 3.1, we have

$$\max_{1 \leq n \leq N} \|\rho^n\| \leq C_1 \|\rho^0\| + C_2 T \cdot \mathcal{O}(\Delta t^{2-\alpha} + h^k + \varepsilon), \quad n = 1, 2, \dots, N,$$

where C_1 and C_2 are two positive constants. Hence we can obtain

$$\max_{1 \leq n \leq N} \|u^n - u_h^n\| \leq \max_{1 \leq n \leq N} \|u^n - P_h u^n\| + \max_{1 \leq n \leq N} \|\rho^n\| = \mathcal{O}(\Delta t^{2-\alpha} + h^k + \varepsilon),$$

with $P_h u^0 = u_h^0$, as required statement. \square

For the convergence analysis of full discrete scheme (19) involving fourth-order CDM, we just state some results as follows. The similar proof can be seen in [20], here we will omit it.

Theorem 3.3. *Let $Q_h : C(\bar{\Omega}) \rightarrow \Omega_h$ be grid projection operator, and $Q_h u = \{u(x) : x \in \Omega_h\}$ with a rectangular grid Ω_h of the closure $\bar{\Omega}$. If $u(t) \in C^6(\Omega)$, then it holds*

$$\left\| Q_h (-\Delta + \gamma\mathbb{I})^s u(t) - (M^{-1}S + \gamma I)^s Q_h u(t) \right\|_{0,h} \leq Ch^4, \quad t > 0,$$

where $\|\cdot\|_{0,h}$ is discrete L^2 norm, and C is a positive constant.

Theorem 3.4. *Under the assumptions of Lemma 3.1 and Theorem 3.3, the full discrete scheme (19), which is based on fourth-order CDM in space, enjoys $\mathcal{O}(\Delta t^{2-\alpha} + h^4 + \varepsilon)$ optimal convergence in maximum norm.*

4. Numerical experiments

In this section, several numerical examples are delivered to test the performance of the presented fast solvers for time-space fractional diffusion equation with spectral fractional Laplacian. And all numerical simulations are conducted using Python 3.7 on the personal computer.

4.1. Accuracy test

To check the accuracy and efficiency of the presented two solvers for spectral fractional Laplacian, we first study the high dimensional fractional Poisson problem (5). Unless otherwise specified, the spatial domain $\Omega = (0, 1)^d$, $\mathcal{N} = N_1 = N_2 = \dots = N_d$ and $h = \mathcal{N}^{-1}$ are given throughout numerical section, and $\mathbf{x} = (x_1, x_2, \dots, x_d)$ for $d = 2, 3$.

From the definition of $(-\Delta + \gamma\mathbb{I})^s$, replace j with (i_1, i_2, \dots, i_d) in (4), which will be convenient when we construct the exact solution. Hence the exact solution of (5) can be easily expressed as

$$u(\mathbf{x}) = \sum_{i_1, i_2, \dots, i_d=1}^{\infty} (\lambda_{i_1, i_2, \dots, i_d} + \gamma)^{-s} \widehat{f}_{i_1, i_2, \dots, i_d} \varphi_{i_1, i_2, \dots, i_d}(\mathbf{x}), \quad \forall \mathbf{x} \in \bar{\Omega}, \quad (32)$$

where the coefficients

$$\widehat{f}_{i_1, i_2, \dots, i_d} = \int_{\Omega} f(\mathbf{x}) \varphi_{i_1, i_2, \dots, i_d}(\mathbf{x}) d\mathbf{x}, \quad i_1, i_2, \dots, i_d \in \mathbb{N}^+.$$

Table 1: The L^2 error and the corresponding convergence rate of Example 1 in linear FEM.

(s, γ)	\mathcal{N}	$\ e_h\ _2$	r_2	(s, γ)	\mathcal{N}	$\ e_h\ _2$	r_2	(s, γ)	\mathcal{N}	$\ e_h\ _2$	r_2
(0.4,0)	8	1.746E-02		(0.8,1)	8	2.365E-03		(1.0,2)	8	8.639E-04	
	16	3.908E-03	2.160		16	5.332E-04	2.149		16	1.955E-04	2.144
	32	9.507E-04	2.039		32	1.300E-04	2.037		32	4.770E-05	2.035
	64	2.361E-04	2.010		64	3.229E-05	2.009		64	1.185E-05	2.009
	128	5.892E-05	2.002		128	8.059E-06	2.002		128	2.959E-06	2.002
256	1.472E-05	2.001	256	2.014E-06	2.001	256	7.394E-07	2.001			
(1.2,0)	8	3.218E-04		(1.6,1)	8	4.282E-05		(2.0,2)	8	5.628E-06	
	16	7.312E-05	2.138		16	9.802E-06	2.127		16	1.297E-06	2.117
	32	1.786E-05	2.034		32	2.398E-06	2.031		32	3.179E-07	2.029
	64	4.438E-06	2.008		64	5.962E-07	2.008		64	7.909E-08	2.007
	128	1.108E-06	2.002		128	1.489E-07	2.002		128	1.975E-08	2.002
256	2.769E-07	2.001	256	3.720E-08	2.001	256	4.936E-09	2.001			

Table 2: The L^2 error and the corresponding convergence rate of Example 1 in fourth-order CDM.

(s, γ)	\mathcal{N}	$\ e_h\ _2$	r_2	(s, γ)	\mathcal{N}	$\ e_h\ _2$	r_2	(s, γ)	\mathcal{N}	$\ e_h\ _2$	r_2
(0.3,0)	8	4.113E-05		(0.5,1)	8	2.606E-05		(0.7,2)	8	6.550E-07	
	16	2.525E-06	4.026		16	1.599E-06	4.026		16	4.017E-08	4.027
	32	1.571E-07	4.007		32	9.949E-08	4.007		32	2.499E-09	4.007
	64	9.806E-09	4.002		64	6.211E-09	4.002		64	1.560E-10	4.002
	128	6.127E-10	4.000		128	3.881E-10	4.000		128	9.748E-12	4.000
256	3.829E-11	4.000	256	2.425E-11	4.000	256	6.092E-13	4.000			
(1.3,0)	8	1.506E-06		(1.5,1)	8	6.550E-07		(1.7,2)	8	1.382E-05	
	16	9.238E-08	4.027		16	4.017E-08	4.027		16	8.481E-07	4.026
	32	5.747E-09	4.007		32	2.499E-09	4.007		32	5.276E-08	4.007
	64	3.588E-10	4.002		64	1.560E-10	4.002		64	3.294E-09	4.002
	128	2.242E-11	4.000		128	9.748E-12	4.000		128	2.058E-10	4.000
256	1.401E-12	4.000	256	6.092E-13	4.000	256	1.286E-11	4.000			

Besides, we choose the eigenpairs $\{(\lambda_{i_1, i_2, \dots, i_d}, \varphi_{i_1, i_2, \dots, i_d})\}$ of the d -dimensional classical Laplacian operator $(-\Delta)$ as following

$$\lambda_{i_1, i_2, \dots, i_d} = \pi^2 \sum_{k=1}^d i_k^2, \quad \text{and} \quad \varphi_{i_1, i_2, \dots, i_d}(\mathbf{x}) = 2 \prod_{k=1}^d \sin(i_k \pi x_k), \quad i_1, i_2, \dots, i_d \in \mathbb{N}^+.$$

We also note from (32) that the exact solution $u(\mathbf{x})$ can be constructed by taking appropriate $f(\mathbf{x})$.

Example 1. (Smooth solution) In equation (5), taking $f(\mathbf{x}) = \prod_{k=1}^d \sin(n\pi x_k)$ leads to

$$\hat{f}_{i_1, i_2, \dots, i_d} = \frac{1}{2} \prod_{k=1}^d \left(\frac{\sin(n\pi - i_k \pi)}{n\pi - i_k \pi} - \frac{\sin(n\pi + i_k \pi)}{n\pi + i_k \pi} \right), \quad n \in \mathbb{N}^+.$$

It can be found that $\hat{f}_{i_1, i_2, \dots, i_d}$ is $\frac{1}{2}$ in the sense of limitation if $i_1 = i_2 = \dots = i_d = n$; otherwise, it will vanish. Hence we have from (32) that

$$u(\mathbf{x}) = \frac{1}{(dn^2\pi^2 + \gamma)^s} \prod_{k=1}^d \sin(n\pi x_k), \quad n \in \mathbb{N}^+.$$

In Example 1, we take $n = 2$ and $d = 3$. The error is measured by $\|e_h\|_2 = \|u - u_h\|_2$ in L^2 norm, and the convergence rate is measured by $r_2 = \log_2 \left(\frac{\|e_h\|_2}{\|e_{h/2}\|_2} \right)$. Hence the expected accuracy is second order in linear FEM, and the expected accuracy is fourth order in CDM. The results are shown in Tables 1 and 2.

Example 2. (*Singular solution*) Let $f(\mathbf{x}) = 1$, $\gamma = 1$ and $d = 2$ in (5).

Table 3: The L^2 error and the convergence rate of Example 2 in FEM and CDM.

s	\mathcal{N}	FEM	r_2	CDM	r_2	s	\mathcal{N}	FEM	r_2	CDM	r_2
0.5	64	3.996E-04		3.039E-04		0.9	64	1.984E-05		4.232E-05	
	128	1.377E-04	1.537	1.089E-04	1.480		128	4.935E-06	2.008	1.098E-05	1.946
	256	4.798E-05	1.521	3.879E-05	1.490		256	1.231E-06	2.003	2.810E-06	1.966
	512	1.682E-05	1.512	1.376E-05	1.495		512	3.075E-07	2.001	7.131E-07	1.979
	1024	5.920E-06	1.507	4.873E-06	1.498		1024	7.684E-08	2.001	1.800E-07	1.986
	2048	2.088E-06	1.504	1.725E-06	1.499		2048	1.921E-08	2.000	4.528E-08	1.991
1.3	64	3.649E-06		1.007E-05		1.7	64	5.738E-07		2.860E-06	
	128	9.124E-07	2.000	2.524E-06	1.997		128	1.436E-07	1.999	7.155E-07	1.995
	256	2.281E-07	2.000	6.313E-07	1.999		256	3.590E-08	2.000	1.789E-07	2.000
	512	5.702E-08	2.000	1.579E-07	2.000		512	8.976E-09	2.000	4.473E-08	2.000
	1024	1.425E-08	2.000	3.947E-08	2.000		1024	2.244E-09	2.000	1.118E-08	2.000
	2048	3.563E-09	2.000	9.867E-09	2.000		2048	5.610E-10	2.000	2.796E-09	2.000

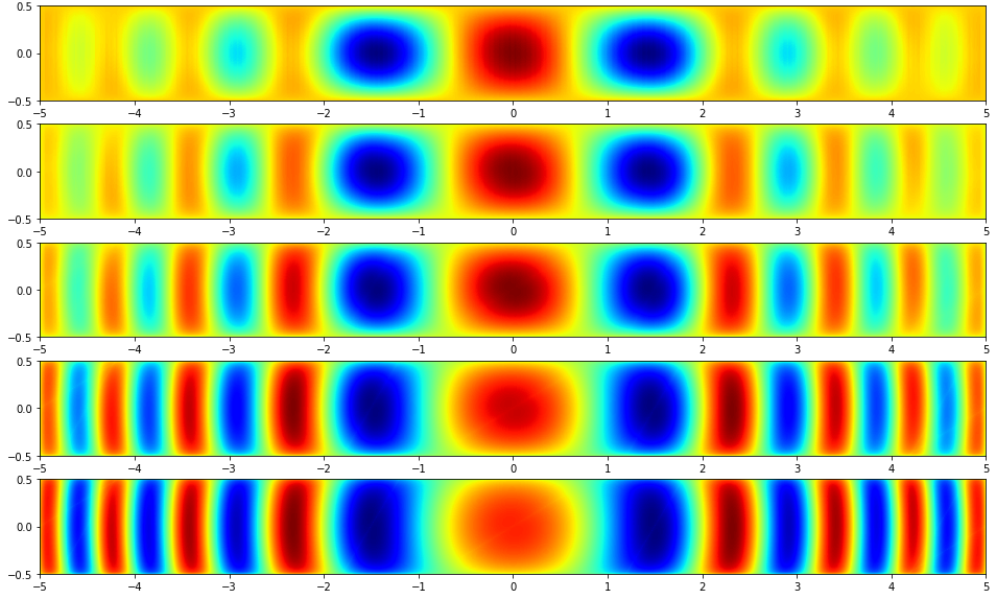


Figure 1: The profiles of the numerical solutions of Example 3 in stripe domain with $s = 0.8, 0.6, 0.4, 0.2, 0.1$ from top to bottom, respectively.

In Example 2, the L^2 error can be measured as $\|e_h\|_2 = \|u_h - u_{h/2}\|_2$, the convergence rate $r_2 = \log_2 \left(\frac{\|e_h\|_2}{\|e_{h/2}\|_2} \right)$, and the expected accuracy is $\mathcal{O}(h^{2s+\frac{1}{2}})$ and $\mathcal{O}(h^2)$ for $s < 0.75$ and $s \geq 0.75$, respectively. The numerical results are presented in Table 3, and the numerical accuracy is consistent with [12]. It is noteworthy that the error is measured in L^2 norm, however, the numerical accuracy will be $\mathcal{O}(h^{2s})$ if the error is measured in maximum norm.

Example 3. In (5), consider the stripe domain $\Omega = (-5, 5) \times (-0.5, 0.5)$, and take

$$f(\mathbf{x}) = 2^{2s}\Gamma(1+s) \left(\cos^{\frac{2s}{5}}(\mathbf{a} \cdot \mathbf{x}) + \sin^{\frac{2s}{5}}(\mathbf{b} \cdot \mathbf{x}) \right) \left(\cos(-|\mathbf{x}|^2) + \frac{6}{5}\sin(-|\mathbf{x}|^2) \right),$$

where $\mathbf{a} = (-\frac{\pi}{3}, \frac{\pi}{5})$ and $\mathbf{b} = (\frac{\pi}{5}, -\frac{\pi}{3})$.

Table 4: The spatial numerical error and the convergence rate of Example 4 in maximum norm.

(s, α)		\mathcal{N}				
		5	10	20	40	80
(1.0, 0.8)	$\ e_h\ _\infty$	1.650E-05	1.127E-06	7.021E-08	4.385E-09	2.740E-10
	r_∞		3.872	4.004	4.001	4.000
(0.8, 0.8)	$\ e_h\ _\infty$	1.747E-05	1.193E-06	7.437E-08	4.645E-09	2.902E-10
	r_∞		3.872	4.004	4.001	4.000
(0.8, 0.6)	$\ e_h\ _\infty$	1.861E-05	1.271E-06	7.920E-08	4.947E-09	3.090E-10
	r_∞		3.872	4.004	4.001	4.001
(0.6, 0.6)	$\ e_h\ _\infty$	1.730E-05	1.182E-06	7.363E-08	4.598E-09	2.872E-10
	r_∞		3.872	4.004	4.001	4.001
(0.6, 0.4)	$\ e_h\ _\infty$	1.869E-05	1.277E-06	7.955E-08	4.966E-09	3.087E-10
	r_∞		3.872	4.004	4.002	4.008
(0.4, 0.4)	$\ e_h\ _\infty$	1.459E-05	9.969E-07	6.212E-08	3.876E-09	2.386E-10
	r_∞		3.872	4.004	4.002	4.022

In Example 3, $\gamma = 0$, $d = 2$, $N_1 = 20000$ and $N_2 = 2000$ are fixed in our numerical simulation, and the fourth-order CDM is used in space. The profiles of the numerical solutions are presented in Figure 1, and we can observe that the change of the profiles is significant from $s = 1$ to $s = 0$.

4.2. Time-dependent problems

In this subsection, we will apply the double fast algorithms to time-space fractional diffusion problems. The fast time stepping $L1$ method based on trapezoidal rule is considered in the simulations. In this experiments, we take $Q = 128$, $w_j = -\frac{\sin(\alpha\pi)}{\pi}\Delta y e^{(1+\alpha)y_j}$, $\xi_j = -e^{y_j}$, $y_j = y_{\min} + j\Delta y$, $\Delta y = \frac{y_{\max} - y_{\min}}{Q-1}$, $y_{\min} = (1+\alpha)^{-1}\log(\varepsilon_0) - \log(T)$, $y_{\max} = \log\left(\frac{-\log(\varepsilon_0) + (1+\alpha)\log(\Delta t)}{0.5\Delta t}\right)$ and $\varepsilon_0 = 10^{-16}$ [30, 31].

Example 4. Let g be time-dependent smooth function, and assume that the exact solution of (2)

$$u(\mathbf{x}, t) = \frac{g(t)}{(dn^2\pi^2 + \gamma)^s} \prod_{k=1}^d \sin(n\pi x_k), \quad n \in \mathbb{N}^+,$$

is chosen so that

$$f(\mathbf{x}, t) = \left(\frac{\partial_t^\alpha g(t)}{(dn^2\pi^2 + \gamma)^s} + \kappa_s g(t) \right) \prod_{k=1}^d \sin(n\pi x_k), \quad n \in \mathbb{N}^+.$$

In Example 4, we take $d = 2$, $\gamma = 1$, $n = 1$, $\kappa_s = 0.1$ and $T = 1$. In addition, the numerical error is measured in L^∞ norm and the spatial numerical method is CDM. The spatial numerical results are presented in Table 4 with $g(t) = t$, temporal mesh $N = 5000$ is fixed, and the expected accuracy is $\mathcal{O}(h^4)$ in space. The temporal numerical results are shown in Table 5 with $g(t) = t^{1.5}$, spatial mesh $\mathcal{N} = 500$ is taken, and the expected accuracy is $\mathcal{O}(\Delta t^{2-\alpha})$ in time.

Table 5: The temporal numerical error and the convergence rate of Example 4 in maximum norm.

(s, α)		N				
		20	40	80	160	320
(1.0, 0.8)	$\ e_h\ _\infty$	1.963E-04	8.601E-05	3.761E-05	1.643E-05	7.168E-06
	r_∞		1.190	1.193	1.195	1.197
(0.8, 0.8)	$\ e_h\ _\infty$	5.746E-04	2.540E-04	1.117E-04	4.894E-05	2.140E-05
	r_∞		1.178	1.186	1.190	1.193
(0.8, 0.6)	$\ e_h\ _\infty$	2.013E-04	7.723E-05	2.951E-05	1.125E-05	4.280E-06
	r_∞		1.382	1.388	1.392	1.394
(0.6, 0.6)	$\ e_h\ _\infty$	5.165E-04	1.993E-04	7.643E-05	2.920E-05	1.113E-05
	r_∞		1.374	1.383	1.388	1.392
(0.6, 0.4)	$\ e_h\ _\infty$	1.653E-04	5.583E-05	1.874E-05	6.258E-06	2.084E-06
	r_∞		1.566	1.575	1.582	1.586
(0.4, 0.4)	$\ e_h\ _\infty$	3.802E-04	1.288E-04	4.333E-05	1.450E-05	4.833E-06
	r_∞		1.561	1.572	1.579	1.585

Example 5. In the example, we study the coarsening dynamics of the following time-space fractional Cahn-Hilliard equation

$$\begin{cases} \partial_t^\alpha u(\mathbf{x}, t) = -(-\Delta)^\beta (\epsilon^{2s} (-\Delta)^s u(\mathbf{x}, t) + F(u)), & \mathbf{x} \in \Omega, t > 0, \\ u(\mathbf{x}, t) = 0, & \mathbf{x} \in \partial\Omega, t \geq 0, \\ u(\mathbf{x}, 0) = u_0(\mathbf{x}), & \mathbf{x} \in \Omega, \end{cases}$$

where $u_0(\mathbf{x})$ is a given initial value, $F(u) = (u^3 - u)$, $0 \leq s, \beta \leq 1$ and $\epsilon > 0$.

In Example 5, a fast time stepping $L1$ method is used for time discretization, and the linear FEM for the spatial discretization is performed. For simplicity, we fix $\beta = 1$, take $\Omega = (0, 1)^2$, and choose initial value as a random perturbation uniformly distributed in $[-0.05, 0.05]^2$, i.e., $u_0(\mathbf{x}) = \text{random}[-0.05, 0.05]^2$. In addition, we take $\epsilon = 0.02$, the time step size $\Delta t = 0.001$ and uniform space step size $h = 2^{-9}$.

We consider different (s, α) to study the effect on coarsening behavior of the time-space fractional Cahn-Hilliard equation. Figure 2 shows the snapshots of the numerical solution at different time $t = 0.026, 0.06, 0.16, 0.5$ when $(s, \alpha) = (0.8, 0.8), (0.8, 0.6), (0.6, 0.6)$ and $(0.6, 0.4)$ from first row to last row, respectively. In this figure, the initial values of four groups simulations are same. We can find that the change of the states of solutions is significant, and the solutions will converge to different steady states for different values of α . Some similar simulations can be seen in [33]. Significantly, the proposed fast algorithm can efficiently simulate the time-space fractional Cahn-Hilliard equation.

5. Conclusion

To explore the high dimensional numerical simulations of time-space fractional diffusion problem, two fast and accurate solvers, which were based on linear finite element method and fourth-order compact difference method combined with matrix transfer technique, were developed in this presented work. In addition, a fast time stepping $L1$ method was applied in the temporal direction. The proposed solvers not only could efficiently overcome the nonlocal nature of fractional differential operators, but also could exactly carry out the derived matrix-vector multiplication by directly using a discrete sine transform and its inverse transform, which didn't need to resort to any iteration method and could significantly reduce computation cost and memory. Besides, the convergence analyses of full discrete scheme based on two types of spatial numerical methods were studied. Finally, some numerical simulations were offered to verify our analyses.

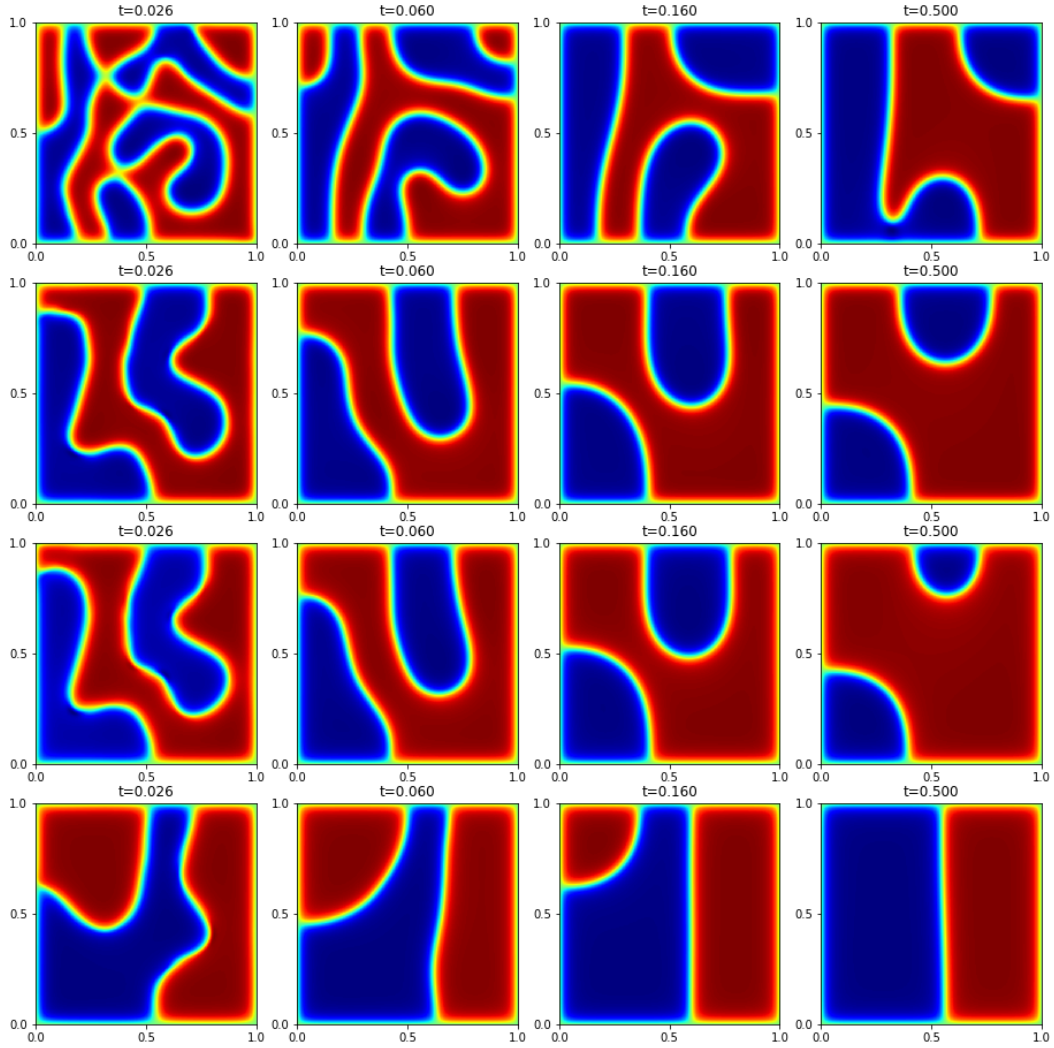


Figure 2: The snapshots of the numerical solution of time-space fractional Cahn-Hilliard equation with $(s, \alpha) = (0.8, 0.8)$, $(0.8, 0.6)$, $(0.6, 0.6)$, $(0.6, 0.4)$ from top to bottom, respectively.

Acknowledgments

This work has been submitted.

References

- [1] J. Klafter and I.M. Sokolov. Anomalous diffusion spreads its wings. *Phys. World*, 18:29–32, 2005.
- [2] C. Bucur and E. Valdinoci. *Nonlocal diffusion and applications*. Springer, 2016.
- [3] S.W. Duo, H. Wang, and Y.Z. Zhang. A comparative study on nonlocal diffusion operators related to the fractional Laplacian. *Discrete. Cont. Dyn.-B.*, 24:231–256, 2019.
- [4] Q. Du. *Nonlocal Modeling, Analysis, and Computation*. Society for Industrial and Applied Mathematics, Philadelphia, PA, 2019.
- [5] W.H. Deng, R. Hou, W.L. Wang, and P.B. Xu. *Modeling Anomalous Diffusion: From Statistics to Mathematics*. World Scientific, Singapore, 2020.
- [6] R. Metzler and J. Klafter. The random walk’s guide to anomalous diffusion: a fractional dynamics approach. *Physics Reports*, 339(1):1–77, 2000.

- [7] W.H. Deng, B.Y. Li, W.Y. Tian, and P.W. Zhang. Boundary problems for the fractional and tempered fractional operators. *Multiscale Model. Sim.*, 16(1):125–149, 2018.
- [8] R. Song and Z. Vondracek. Potential theory of subordinate killed Brownian motion in a domain. *Probab. Theory Relat. Fields.*, 125(4):578–592, 2003.
- [9] R.H. Nochetto, E. Otárola, and A.J. Salgado. A PDE approach to fractional diffusion in general domains: a priori error analysis. *Found. Comput. Math.*, 15(3):733–791, 2015.
- [10] X. Liu and W.H. Deng. Numerical approximation for fractional diffusion equation forced by a tempered fractional Gaussian noise. *J. Sci. Comput.*, 84, 2020.
- [11] Q.Q. Yang, I. Turner, F.W. Liu, and M. Ilic. Novel numerical methods for solving the time-space fractional diffusion equation in two dimensions. *SIAM J. Sci. Comput.*, 33(3):1159–1180, 2011.
- [12] S.W. Duo, L.L. Ju, and Y.Z. Zhang. A fast algorithm for solving the space-time fractional diffusion equation. *Comput. Math. Appl.*, 75:1929–1941, 2018.
- [13] A. Bonito, J.P. Borthagaray, R.H. Nochetto, E. Otárola, and A.J. Salgado. Numerical methods for fractional diffusion. *Comput. Vis. Sci.*, 19:19–46, 2018.
- [14] S. Chen and J. Shen. An efficient and accurate numerical method for the spectral fractional Laplacian equation. *J. Sci. Comput.*, 82:1–25, 2020.
- [15] A. Bonito and J.E. Pasciak. Numerical approximation of fractional powers of elliptic operators. *Math. Comput.*, 84:2083–2110, 2015.
- [16] S. Harizanov, R.D. Lazarov, P. Marinov, S. Margenov, and J.E. Pasciak. Analysis of numerical methods for spectral fractional elliptic equations based on the best uniform rational approximation. *arXiv preprint arXiv:1905.08155*, 2019.
- [17] S. Harizanov, R.D. Lazarov, S. Margenov, and P. Marinov. *The best uniform rational approximation: application to solving equations involving fractional powers of elliptic operators*. arXiv preprint arXiv:1910.13865, 2019.
- [18] S. Harizanov, R. Lazarov, S. Margenov, and P. Marinov. Numerical solution of fractional diffusion-reaction problems based on BURA. *Comput. Math. Appl.*, 2019.
- [19] M. Ilic, F. Liu, I. Turner, and V. Anh. Numerical approximation of a fractional-in-space diffusion equation, I. *Fract. Calc. Appl. Anal.*, 8(3):323–341, 2005.
- [20] B.J. Szekeres and F. Izsák. Finite difference approximation of space-fractional diffusion problems: the matrix transformation method. *Comput. Math. Appl.*, 73(2):261–269, 2017.
- [21] G. Maros and F. Izsák. Finite element methods for fractional-order diffusion problems with optimal convergence order. *Comput. Math. Appl.*, 80:2105–2114, 2020.
- [22] B.J. Szekeres and F. Izsák. Finite element approximation of fractional order elliptic boundary value problems. *J. Comput. Appl. Math. (2016)*, 292:553–561, 2016.
- [23] M.L. Zheng, Z.M. Jin, F.W. Liu, and V. Anh. Matrix transfer technique for anomalous diffusion equation involving fractional Laplacian. *Appl. Numer. Math.*, 172:242–258, 2022.
- [24] C.T. Sheng, D. Cao, and J. Shen. Efficient spectral methods for PDEs with spectral fractional Laplacian. *J. Sci. Comput.*, 88, 2021.
- [25] F. Izsák and B.J. Szekeres. Efficient computation of matrix power-vector products: Application for space-fractional diffusion problems. *Appl. Math. Lett.*, 86:70–76, 2018.
- [26] L. Ju, J. Zhang, L. Zhu, and Q. Du. Fast explicit integration factor methods for semilinear parabolic equations. *J. Sci. Comput.*, 62:431–455, 2015.
- [27] L. Zhu, L. Ju, and W.D. Zhao. Fast high-order compact exponential time differencing Runge-Kutta methods for second-order semilinear parabolic equations. *J. Sci. Comput.*, 67:1043–1065, 2016.
- [28] S.D. Jiang, J.W. Zhang, Q. Zhang, and Z.M. Zhang. Fast evaluation of the Caputo fractional derivative and its applications to fractional diffusion equations. *Commun. Comput. Phys.*, 21(3):650–678, 2017.
- [29] Y.G. Yan, Z.Z. Sun, and J.W. Zhang. Fast evaluation of the Caputo fractional derivative and its applications to fractional diffusion equations: a second-order scheme. *Commun. Comput. Phys.*, 22(4):1028–1048, 2017.
- [30] Y.X. Huang, Q.G. Li, R.X. Li, F.H. Zeng, and L. Guo. A unified fast memory-saving time-stepping method for fractional operators and its applications. *Numer. Math. Theor. Meth. Appl.*, 2022.
- [31] Y.X. Huang, F.H. Zeng, and L. Guo. Error estimate of the fast L1 method for time-fractional subdiffusion equations. *Appl. Math. Lett.*, 2022.
- [32] K. Sakamoto and M. Yamamoto. Initial value/boundary value problems for fractional diffusion-wave equations and applications to some inverse problems. *J. Math. Anal. Appl.*, 382:426–447, 2011.
- [33] L.L. Bu, L.Q. Mei, and Y. Hou. Stable second-order schemes for the space-fractional Cahn-Hilliard and Allen-Cahn equations. *Comput. Math. Appl.*, 78:3485–3500, 2019.